SOS1 Gain of Function Variants in Dilated Cardiomyopathy

Running title: *Cowan et al.; SOS1 variants in dilated cardiomyopathy*

Jason R. Cowan, PhD[1,2]; Lorien Salyer, BS[1,2]; Nathan T. Wright, PhD[4];

Daniel D. Kinnamon, PhD[1,2]; Pedro Amaya, BS[1,2]; Elizabeth Jordan, MS, LGC[1,2];

University of Washington Center for Mendelian Genomics; Michael Bamshad, MD[5,6];

Deborah A. Nickerson, PhD[5]; Ray E. Hershberger, MD[1-3,7,]

[1]Dorothy M. Davis Heart and Lung Research Institute, [2]Divisions of Human Genetics and [3]Cardiovascular Medicine, Department of Internal Medicine at The Ohio State University College of Medicine, Columbus, OH; [4]Department of Chemistry and Biochemistry, James Madison University, Harrisonburg, VA; [5]Department of Pediatrics, [6]Department of Genome Sciences, University of Washington, Seattle, WA

Correspondence:

Ray E. Hershberger, MD

Ohio State University,

460 West 12th Avenue

Biomedical Research Tower Room 304

Columbus, OH 43210

Tel: 614-688-1305

Fax: 614-688-1381

E-mail: Ray.Hershberger@osumc.edu

Journal Subject Terms: Cardiomyopathy; Heart Failure; Genetics

Abstract:

Background - Dilated cardiomyopathy (DCM) is a genetically heterogeneous cardiac disease characterized by progressive ventricular enlargement and reduced systolic function. Here, we report genetic and functional analyses implicating the RAS signaling protein, SOS1, in DCM pathogenesis.

Methods - Exome sequencing was performed on 412 probands and family members from our DCM cohort, identifying several *SOS1* variants with potential disease involvement. As several lines of evidence have implicated dysregulated RAS signaling in the pathogenesis of DCM, we assessed functional impact of each variant on activation of ERK, AKT, and JNK pathways. Relative expression levels were determined by western blot in HEK293T cells transfected with variant or wild-type human *SOS1* expression constructs.

Results - A rare *SOS1* variant [c.571G>A, p.(Glu191Lys)] was found to segregate alongside an A-band Titin (*TTN*) truncating variant in a pedigree with aggressive, early onset DCM. Reduced disease severity in the absence of the *SOS1* variant suggested its potential involvement as a genetic risk factor for DCM in this family. Exome sequencing identified five additional *SOS1* variants with potential disease involvement in four other families [c.1820T>C, p.(Ile607Thr); c.2156G>C, p.(Gly719Ala); c.2230A>G, p.(Arg744Gly); c.2728G>C, p.(Asp910His); c.3601C>T, p.(Arg1201Trp)]. Impacted amino acids occupied a number of functional domains relevant to SOS1 activity, including the N-terminal histone fold (HF), as well as the C-terminal RAS-exchange motif (REM), CDC25, and proline-rich (PR) tail domains. Increased pERK expression relative to wild-type levels was seen for all six *SOS1* variants, paralleling known disease-relevant *SOS1* signaling profiles.

Conclusions - These data support gain of function variation in *SOS1* as a contributing factor to isolated DCM.

Key words: dilated cardiomyopathy; genetics; genetic heart disease; SOS1 protein; son of sevenless protein

Nonstandard Abbreviations and Acronyms:

AKT	Protein kinase B
ACMG	American College of Medical Genetics
CFCS	Cardiofaciocutaneous syndrome
ClinGen	Clinical Genome Resource
DH	Dbl homology
DCM	Dilated cardiomyopathy
LVEF	Left ventricular ejection fraction
EGF	Epidermal growth factor
ERK	Extracellular signal-regulated kinase
ExAC	Exome Aggregation Consortium (ExAC)
FLNC	Filamin C
GEF	Guanine exchange factor
gnomAD	Genome Aggregation Database
GRB2	Growth factor receptor-bound protein 2
HCM	Hypertrophic cardiomyopathy
HGMD	Human Gene Mutation Database
HF	Histone-like fold
ICD	Implantable cardioverter defibrillator
JNK	c-Jun N-terminal kinase
LMNA	Lamin A/C
MAPK	Mitogen-activated protein kinase
MIM	Mendelian Inheritance in Man
MYH6	Myosin heavy chain 6
NMR	Nuclear magnetic resonance
NS	Noonan syndrome
PDB	Protein Data Bank
PH	Pleckstrin homology
PPCM	Peripartum cardiomyopathy
PR	Proline-rich
PTPN11	Tyrosine-protein phosphatase non-receptor type 11
REM	RAS-exchange motif
SOS1	Son of Sevenless
SYNE1	Nesprin-1
TTN	Titin
TTNtv	Titin truncating variant
VUS	Variant of uncertain significance
WPW	Wolff-Parkinson-White

Introduction

To date, over 50 genes have been identified as causative or likely causative for dilated cardiomyopathy (DCM)[1, 2]. While identification of these genes has greatly improved our understanding of the genetic basis for DCM, low diagnostic yields (~37%) of clinical genetic testing panels[3] support existence of additional undiscovered genetic causes.

The impetus for the present study originated from identification of a rare Son of Sevenless 1 (*SOS1)* variant segregating in three severely affected individuals of a large family with early-onset, bilineal DCM (Figure 1A). Exome sequencing of our wider DCM cohort identified a further five *SOS1* variants of potential pathogenic significance spanning four additional families (Figure 1B-E). We considered SOS1, a RAS-activating guanine exchange factor (GEF), to be a plausible DCM candidate as animal and human data have previously implicated dysregulated RAS signaling in the pathogenesis of DCM[4-8].

Befitting critical roles for mitogen-activated protein kinase (MAPK) signaling pathways in cardiac development, remodeling, and disease[9], *SOS1* variants underlie a number of cardiovascular genetic disorders, including Noonan syndrome (NS, Mendelian Inheritance in Man (MIM): 610733), and cardiofaciocutaneous syndrome (CFCS, MIM: 115150). Myocardial involvement is a well-recognized component and while hypertrophic cardiomyopathy (HCM) is more common, DCM has also been reported, including in one patient carrying a p.(Met269Thr) *SOS1* variant[10]. Supporting involvement of *SOS1* in non-syndromic disease, targeted sequencing of RAS signaling genes have identified a number of *SOS1* variants with possible pathogenic potential in patients with isolated cardiomyopathy[11-13].

Clinically-relevant *SOS1* variants typically promote increased GEF activity and hyperactivation of downstream RAS effectors[14, 15]. This proclivity towards gain of function

effect is directly related to the structure of the SOS1 protein, which natively exists in an auto-inhibited state governed by complex interplay between six distinct functional domains (Figure 2)[16-19]. Pathogenic variants disrupt these interactions, promoting sustained RAS activation[20]. Three N-terminal domains - a histone-like fold (HF) domain, a Dbl homology (DH) domain, and a pleckstrin homology (PH) domain - comprise an auto-inhibitory unit that orients to prevent RAS binding when SOS1 is not associated with the plasma membrane[17, 18] (Figure 2A). Membrane association is primarily driven through direct interaction of the proline-rich (PR) tail with Growth factor receptor-bound protein 2 (GRB2)[21] while secondary associations are provided by the HF[16, 18], and PH[22] domains (Figure 2B). Two additional domains: a RAS-exchange motif (REM) and a CDC25 domain, collectively comprise the C-terminal SOS1 catalytic core. The latter domain serves as the site of GDP/GTP exchange and the former as a non-substrate RAS binding site[23]. When SOS1 is unbound, the DH-PH regulatory unit blocks access of RAS to the REM binding site[16, 19] (Figure 2A). Alleviation of auto-inhibition on membrane association frees the REM to bind to RAS, initiating conformational changes that promote binding of a second RAS molecule at the adjacent CDC25 catalytic site (Figure 2B). These structural rearrangements create a positive feedback loop whereby activated RAS from the CDC25 domain can rebind the REM, facilitating further RAS recruitment and activation[23]. The complexity of these intramolecular interactions provides ample opportunity for genetic disruption and forms the molecular basis for *SOS1*-related disease.

A simplified overview of RAS signaling pathway components, including SOS1, is shown in Figure 2C alongside known associated disease phenotypes. In this context, we describe genetic and functional analyses of six *SOS1* variants identified in our DCM cohort. Our results provide preliminary evidence for involvement of gain of function *SOS1* variants in isolated DCM

and support consideration of DCM in the phenotypic spectrum of *SOS1*-associated genetic disease.

Methods

Complete study methods are provided in the Supplemental Materials. The sequencing and analytical data are available to other researchers upon request for confirmation and/or replication of our analysis. Informed consent was obtained from all study participants following Institutional Review Board approval by the Oregon Health & Science University, the University of Miami, or the Ohio State University.

Results

Exome sequencing of 412 total individuals from our DCM cohort, including 281 probands and 131 of their affected family members, identified six heterozygous missense *SOS1* variants of possible pathogenicity segregating in five families of non-Hispanic, European ancestry (Figure 1, Table 1).

All six *SOS1* variants were considered to be variants of uncertain significance (VUSs) using refined guidelines for DCM variant interpretation[24]. The five families included 1 simplex and 4 multiplex (i.e., affected members spanning multiple generations) families. DNA was unavailable in some individuals who were reported to be affected. In 2 families (Pedigrees A and E), exome sequencing identified additional rare variants in at least one other known DCM gene. No clinical features consistent with syndromic RASopathies were identified in Families B to E (Table 2). However, presentation of a photograph of Family A (Individuals A.4, A.5, A.6, A.7, A.8) to a research conference of the Department of Molecular and Medical Genetics at the

Oregon Health & Science University elicited spontaneous comments from three medical geneticists that individuals A.7 and A.8, both teenagers at the time the photograph was taken, had facial features consistent with NS.

Pedigree A

A paternally inherited p.(Glu191Lys) variant in *SOS1* predicted to impact the HF domain was identified in a large family with severe, early-onset DCM and arrhythmia (Pedigree A). The *SOS1* variant co-segregated with a truncating A-band *TTNtv* [p.(Val30827Serfs*22)], present in three of the most severely affected family members: (A.4), who died of heart failure at 57 years, and two of his sons (A.7, A.8), both of whom required transplantation at an early age (30 years and 14 years, respectively). An additional son (A.6) with a borderline low left ventricular ejection fraction (LVEF) of 48% but no other indications of DCM carried only the *TTNtv*, suggesting that this variant was unlikely to explain the totality of disease in affected family members. An additional maternally inherited truncating *FLNC* variant [p.(Val1643ThrfsTer26)] was identified in both A.7 and A.8, which also likely contributed to their DCM phenotype even though the remainder of the *FLNC* carriers in the maternal pedigree had less overt disease. Greatest disease severity - DCM requiring transplantation, implantable cardioverter defibrillator (ICD)-placement, or resulting in DCM-related death - was observed in individuals carrying all three variants.

Pedigree B

Two C-terminal *SOS1* variants - p.(Ile607Thr), affecting the REM domain, and p.(Asp910His), impacting the CDC25 domain - were inherited in *cis* in a family with DCM and conduction system disease (Pedigree B). Both variants were carried by the proband (B.4), her severely affected son (B.6), who also had a history of Wolff-Parkinson-White (WPW) syndrome, and her

clinically unaffected and possibly non-penetrant daughter (B.7). One additional family member with advanced DCM, arrhythmia, and a history of Doxorubicin treatment was identified (B.3); however, she did not carry either *SOS1* variant. Because of her medical history, we are unable to rule out drug-induced cardiotoxicity as the cause of her DCM.

Pedigree C

A p.(Gly719Ala) variant predicted to affect the REM catalytic domain was identified in a female proband (C.4) with peripartum cardiomyopathy (PPCM), diagnosed at 25 years (Pedigree C). She underwent mitral valve replacement at 37 years following increasing severity of symptoms associated with mitral regurgitation and congestive heart failure. The proband's father (C.1) died at 70 years from heart failure associated with DCM. DNA and medical records were unavailable for the proband's sister (C.6), who reportedly died at 42 years from sudden cardiac death, as well as for her sister's son (C.7), who was reported to have severe (LVEF~20%) early onset DCM diagnosed at 25 years. Echocardiographic records confirmed a diagnosis of DCM in the proband's other affected sister at 39 years (C.3), but again DNA was unavailable.

Pedigree D

A p.(Arg744Gly) variant predicted to affect the REM domain was identified in a proband (D.5) with severe (Grade IV) DCM (Pedigree D). Family history was significant only for a paternal grandmother with reported heart failure at an early age. No additional family members were available for testing.

Pedigree E

A p.(Arg1201Trp) variant predicted to affect the PR tail domain was identified in two sisters with DCM and arrhythmia (Pedigree E). The proband (E.4) and her sister (E.6) both carried the

SOS1 variant as well as a p.(Glu1926Asn) variant in *MYH6*. Absence of single variant carriers precluded analysis of individual variant impact.

Functional Studies of *SOS1* Variants.

To determine the effect of each variant on RAS signaling pathways, wild-type and variant *SOS1* constructs were expressed in HEK293T cells. Extracellular signal-regulated kinase (ERK), Protein kinase B (AKT), and c-Jun N-terminal kinase (JNK) activations were then determined by western blotting. Phosphorylated ERK (pERK) signals were undetectable in serum-starved cells, but increased following 15 min stimulation with epidermal growth factor (EGF) (Figure 3). Relative to wild-type *SOS1* transfections, estimated fold changes in median pERK expression following 15 min EGF stimulation ranged between 1.5 and 2.1 for all six variants ($p < 0.04$). As expected, comparable increases were observed for both NS-associated variants used as positive controls for ERK activation [p.(Met269Arg) and p.(Glu846Lys)][15, 26] ($p \leq 0.01$), but not for the suspected benign p.(Leu791Ile) variant ($p = 0.36$). In contrast, 95% confidence intervals supported lack of impact of identified SOS1 variants on pAKT (Figure S1) and pJNK (Figure S2) signaling. A <0.5 fold reduction in pJNK activation observed for the p.(Asp910His) variant was considered to be most likely related to reduced SOS1 expression observed in these samples (Figure S2).

Structural Analyses of *SOS1* Variants

We next mapped each variant to crystal structures of native and RAS-bound SOS1 [Protein Data Bank (PDB) IDs: 3KSY, 1NVV] and modeled impact on higher level protein structure. Five of the SOS1 variants map to C-terminal domains, including three [p.(Ile607Thr), p.(Gly719Ala), p.(Arg744Gly)] in the REM, one in the CDC25 [p.(Asp910His)], and one in the PR tail

[p.(Arg1201Trp)] (Figure 4, Figure 5A). One variant [p.(Glu191Lys)] mapped to the N-terminal HF.

The p.(Glu191Lys) variant present in Family A was predicted to impact an unstructured loop bridging the HF and DH domain (Figure 5B). Modeling of the wild-type protein suggests the presence of an intermittent electrostatic association between Glu191 and Lys420 (Figure 5B). This interaction is ablated in p.(Glu191Lys) models. As SOS1 autoinhibition depends on proper orientation of the DH-PH unit relative to the C-terminal catalytic core[19], Glu191 may natively act to provide stability to SOS1 through its association with the PH domain. Introduction of the oppositely charged Lys residue may destabilize the wild-type interaction, shifting the loop away from the PH domain and inducing opening of the allosteric RAS binding site.

Molecular models support distinct structural mechanisms for the REM variants identified in Family B. Asp910 directly associates with Arg41 of the RAS Switch 1 region (Figure 5F)[28] and borders amino acids important for interactions with Switch 2[29]. While exact mechanisms underlying observed gain of function effects are not known, both positive[28, 30] and negative[31] impacts on nucleotide exchange rates have been described for RAS Switch 1 variants, highlighting the functional complexity of RAS-SOS1 interactions in this region. Structural modeling of p.(Ile607Thr) supported a hydrogen bond rearrangement between the region surrounding Ile607 and the neighboring CDC25 helical hairpin (Figure 5C). Specifically, the addition of an –OH group was found to promote interactions between both Arg576-Thr607 and Lys953-Thr607. This linking has the effect of repositioning the CDC25 helical hairpin slightly closer to the REM domain. As this area constitutes the primary interface between the REM and CDC25[28], and acts as a hinge point for paired rotations of the REM and CDC25 following RAS

binding[23, 32], this altered hydrogen bond network may promote exposure of the previously occluded catalytic site[32].

The REM variants detected in Family C [p.(Gly719Ala)] and D [p.(Arg744Gly)] are predicted to occupy adjacent helices bridging the catalytic and allosteric RAS binding domains. Based on this positioning, neither variant was expected to directly interact with the DH domain or with bound RAS. Nevertheless, nuclear magnetic resonance (NMR) studies have suggested involvement of nearby Met714 in dynamic conformational changes following RAS binding[27] (Figure 5D). A functional role for residues of this helix is further supported by elevated ERK signaling and nucleotide exchange rates[33] for p.(Tyr702His), a NS-associated variant located at the REM-CDC25 interface. As Arg744 is similarly positioned, it is plausible that p.(Arg744Gly) may also impact SOS1 function by disrupting allosteric communication between the REM and CDC25. While no further structural insights were gained from molecular modeling of p.(Gly719Ala), p.(Arg744Gly) consistently demonstrated a localized unwinding of the helix about 1 turn earlier than in wild-type models (Figure 5E), suggesting local dynamics of this region may play a role in RAS signaling.

The final SOS1 variant, p.(Arg1201Trp), found in Family E, was predicted to impact a highly conserved residue positioned between the second and third of four GRB2 consensus binding motifs within the PR tail. This region adopts a disordered random-coil confirmation in solution[34] and cannot be accurately modeled using all-atom simulations. Nevertheless, multiple genetic and functional studies support roles for the PR tail in negatively regulating SOS1 activity[35, 36]. Thus, the gain of function effect of the Arg1201Trp mutant, while structurally unexplained, is consistent with known functions of the SOS1 C-terminal domain.

Discussion

Exome sequencing completed on 412 individuals with isolated DCM, including 281 probands and 131 of their affected relatives, identified six *SOS1* coding variants spanning five families. Detected variants were tested for impact on RAS signaling pathways and were found to result in gain of function effects on ERK signaling with minimal impact on AKT and JNK pathways. Activations were of comparable magnitude to those obtained using two NS-associated variants with previously recognized pathogenicity and functional impact (Table S1). These results extend previous studies[4-6] to strengthen the general evidence that dysregulated ERK activation plays a role in pathogenesis of DCM.

This study is one of only a few others[11-13] to directly assess *SOS1* genetic variation in the context of non-syndromic cardiomyopathy. To date, all reported DCM-associated *SOS1* variants, including those reported in this study, have been classified as VUSs (Table S2). Interestingly, several previously reported variants impacted residues located close to functionally significant residues identified in our cohort. In our study, five of six detected *SOS1* variants affected C-terminal residues: three in the REM domain [p.(Ile607Thr), p.(Gly719Ala), p.(Arg744Gly), one in the CDC25 domain [p.(Asp910His)], and one in the PR tail [p.(Arg1201Trp)]. While the limited number of identified variants precludes definitive genotype-phenotype determinations, only 18 of the 60 *SOS1* missense/nonsense variants currently documented in the Human Gene Mutation Database (HGMD), most of which are NS-associated, localize to C-terminal domains.

A role for activated ERK signaling in development of DCM has previously been established by studies of both failing human hearts and mutant mice models[4-6]. A number of these animal models impact genes encoding nuclear envelope proteins with known importance to human DCM, including *LMNA* (lamin A/C) and *SYNE1* (nesprin-1). While the exact mechanisms

underlying ERK activation are uncertain, it has been hypothesized that RAS signaling may be disrupted through effects on nuclear envelope organization and transport rather than through direct influence on upstream signaling components[6]. Evidence supporting an alternative, but not necessarily mutually exclusive, mechanism suggests that hyperactivated pERK can act to alter sarcomeric organization through increased phosphorylation and activation of the actin depolymerization factor, cofillin-1[37]. Whether similar disruption of sarcomere actin dynamics are seen with other ERK activating DCM models outside of *LMNA* remains an untested but important question.

While no consistent changes were seen in AKT and JNK signaling in this study, components of each of these pathways have been reported to be upregulated in dilated human hearts[38, 39]. This broader signaling complexity is further suggested by results from functional models of *RAF1*[8], which implicate AKT activation in development of early onset DCM, and from Tyrosine-protein phosphatase non-receptor type 11 (*Ptpn11)* mouse models, which develop myocardial thinning evocative of DCM in a setting of reduced ERK and elevated AKT[40, 41]. Because DCM is only infrequently seen in NS[42-44], its occurrence in *Ptpn11* mouse models is intriguing. Affected animals develop DCM at 6-8 weeks without any evidence of the cardiac hypertrophy commonly seen in NS. It would be logical to hypothesize that because loss of *Ptpn11* function results in DCM, gain of function variants might be associated with HCM in a manner analogous to knock-in models of NS-associated *Sos1*[45] and *Raf1*[46] variants. However, at least some *Ptpn11* knock-in mice models exhibit myocardial thinning evocative of DCM[40, 41, 47]. These models underscore the fact that we do not yet have a complete picture as to how abnormal ERK signaling acts to promote particular myopathic responses. Recent studies from the Molkentin group[48, 49] have supported a role for increased ERK signaling in concentric

hypertrophy and decreased ERK signaling in eccentric hypertrophy, while others[46, 50] describe pathological eccentric hypertrophy in the context of ERK hyperactivation. One possible explanation for such discrepancies has been raised: ERK activation in other cell types apart from cardiomyocytes is likely to play in a role in shaping the final hypertrophic response. Cardiac fibroblasts, for example, are relevant for cardiomyocyte hypertrophy[51] and Raf1^{L613V} knock-in mice, which express the mutant allele in both cell types, develop an eccentric cardiomyopathy characterized by ERK hyperactivation and correctable by postnatal inhibition[46, 50]. Alongside other emerging studies[52, 53], these data suggest that myocyte-focused views of hypertrophy may be too narrow to adequately explain disease mechanisms underlying RASopathies and their associated cardiomyopathies.

Limitations

Because many study participants were recruited from cardiovascular rather than general genetics clinics, subtle findings suggestive of underlying RASopathies may have been missed during evaluation. While it remains a formal possibility that the *MYH6* p.(Gly1826Asn) variant detected in Family E may be disease-relevant, a definitive role for *MYH6* in DCM has yet to be established and previous reports have considered this variant to be of unlikely or uncertain pathogenic significance[54, 55]. Current American College of Medical Genetics (ACMG) / Clinical Genome Resource (ClinGen) criteria for variant adjudication focus heavily on single-gene Mendelian paradigms[25] and variant classifications will continue to be refined as standards evolve to incorporate a more nuanced understanding of complex disease patterns. It is important to note that ERK activations reported in this study reflect results obtained from a single *in vitro* system. Additional testing using patient samples or other cell or animal based functional assays will be required before activated ERK signaling can be definitively established as a pathogenic

mechanism in these families. Because the identities of precise ERK targets relevant to DCM remain uncertain, these studies will be of great help in determining how aberrant activation of ERK signaling in the heart may differ from pathologic activation in other cell or organ systems.

Conclusions

Our results provide evidence supporting gain of function SOS1 genetic variation as a contributing factor to isolated DCM. Whether the majority of DCM-associated SOS1 variants are sufficient to cause DCM in isolation or more commonly act as genetic modifiers alongside other causative variants remains to be determined. Nevertheless, observed signaling profiles in this study paralleled those previously described for other pathogenic *SOS1* variants. While preliminary, these data reflect a well-recognized but poorly understood role for ERK signaling in DCM. By what cellular mechanisms might signaling changes imparted by *SOS1* variants promote development of DCM? What are the identities of any relevant downstream signaling targets and how might these differ from those involved in other forms of *SOS1*-related RASopathy? As clinical and animal-based trials of pathway-specific MAPK inhibitors have already demonstrated therapeutic potential for treatment of DCM, these questions raise intriguing possibilities for precision-medicine approaches to patient care. Large-scale, family-based DCM studies are underway[56] and will be invaluable in driving novel gene discovery.

Acknowledgments: We thank all probands and family members for their ongoing participation as well as Dr. Benjamin Neel (New York University Medical Center, NYUMC) for providing pBABE-puro expression vectors. This study was supported in part by computational infrastructure provided by The Ohio State University Division of Human Genetics Data Management Platform and the Ohio Supercomputer Center.

Sources of Funding: NIH RO1 HL58626 and R01 HL128857 (both to Dr Hershberger), and 5 M01 RR000334. Sequencing was provided by the University of Washington Center for Mendelian Genomics (UW-CMG) and was funded by National Human Genome Research Institute (NHGRI) and National Heart, Lung, and Blood Institute (NHLBI) grants UM1 HG006493 and U24 HG008956. The content is solely the responsibility of the authors and does not necessarily represent the official views of the National Institutes of Health (NIH).

Disclosures: None.

References.

1. Hershberger RE, Hedges DJ, Morales A. Dilated cardiomyopathy: the complexity of a diverse genetic architecture. *Nat Rev Cardiol*. 2013;10:531-47.

2. McNally EM, Mestroni L. Dilated Cardiomyopathy: Genetic Determinants and Mechanisms. *Circ Res*. 2017;121:731-748.

3. Pugh TJ, Kelly MA, Gowrisankar S, Hynes E, Seidman MA, Baxter SM, Bowser M, Harrison B, Aaron D, Mahanta LM, et al. The landscape of genetic variation in dilated cardiomyopathy as surveyed by clinical DNA sequencing. *Genet Med*. 2014;16:601-8.

4. Muchir A, Pavlidis P, Decostre V, Herron AJ, Arimura T, Bonne G, Worman HJ. Activation of MAPK pathways links LMNA mutations to cardiomyopathy in Emery-Dreifuss muscular dystrophy. *J Clin Invest*. 2007;117:1282-93.

5. Muchir A, Reilly SA, Wu W, Iwata S, Homma S, Bonne G, Worman HJ. Treatment with selumetinib preserves cardiac function and improves survival in cardiomyopathy caused by mutation in the lamin A/C gene. *Cardiovasc Res*. 2012;93:311-9.

6. Zhou C, Li C, Zhou B, Sun H, Koullourou V, Holt I, Puckelwartz MJ, Warren DT, Hayward R, Lin Z, et al. Novel nesprin-1 mutations associated with dilated cardiomyopathy cause nuclear envelope disruption and defects in myogenesis. *Hum Mol Genet*. 2017;26:2258-2276.

7. Arimura T, Helbling-Leclerc A, Massart C, Varnous S, Niel F, Lacene E, Fromes Y, Toussaint M, Mura AM, Keller DI, et al. Mouse model carrying H222P-Lmna mutation develops muscular dystrophy and dilated cardiomyopathy similar to human striated muscle laminopathies. *Hum Mol Genet*. 2005;14:155-69.

8. Dhandapany PS, Razzaque MA, Muthusami U, Kunnoth S, Edwards JJ, Mulero-Navarro S, Riess I, Pardo S, Sheng J, Rani DS, et al. RAF1 mutations in childhood-onset dilated cardiomyopathy. *Nat Genet*. 2014;46:635-639.

9. Rose BA, Force T, Wang Y. Mitogen-activated protein kinase signaling in the heart: angels versus demons in a heart-breaking tale. *Physiol Rev*. 2010;90:1507-46.

10. Baban A, Olivini N, Lepri FR, Cali F, Mucciolo M, Digilio MC, Calcagni G, di Mambro C, Dallapiccola B, Adorisio R, et al. SOS1 mutations in Noonan syndrome: Cardiomyopathies and not only congenital heart defects! Report of six patients including two novel variants and literature review. *Am J Med Genet A*. 2019;179:2083-2090.

11. Ceyhan-Birsoy O, Miatkowski MM, Hynes E, Funke BH, Mason-Suares H. NGS testing for cardiomyopathy: Utility of adding RASopathy-associated genes. *Hum Mutat*. 2018;39:954-958.

12. Aljeaid D, Sanchez AI, Wakefield E, Chadwell SE, Moore N, Prada CE, Zhang W. Prevalence of pathogenic and likely pathogenic variants in the RASopathy genes in patients who have had panel testing for cardiomyopathy. *Am J Med Genet A*. 2019;179:608-614.

13. Kaski JP, Syrris P, Shaw A, Alapi KZ, Cordeddu V, Esteban MT, Jenkins S, Ashworth M, Hammond P, Tartaglia M, et al. Prevalence of sequence variants in the RAS-mitogen activated protein kinase signaling pathway in pre-adolescent children with hypertrophic cardiomyopathy. *Circ Cardiovasc Genet*. 2012;5:317-26.

14. Jang SI, Lee EJ, Hart PS, Ramaswami M, Pallos D, Hart TC. Germ line gain of function with SOS1 mutation in hereditary gingival fibromatosis. *J Biol Chem*. 2007;282:20245-55.

15. Roberts AE, Araki T, Swanson KD, Montgomery KT, Schiripo TA, Joshi VA, Li L, Yassin Y, Tamburino AM, Neel BG, et al. Germline gain-of-function mutations in SOS1 cause Noonan syndrome. *Nat Genet*. 2007;39:70-4.

16. Yadav KK, Bar-Sagi D. Allosteric gating of Son of sevenless activity by the histone domain. *Proc Natl Acad Sci U S A*. 2010;107:3436-40.

17. Corbalan-Garcia S, Margarit SM, Galron D, Yang SS, Bar-Sagi D. Regulation of Sos activity by intramolecular interactions. *Mol Cell Biol*. 1998;18:880-6.

18. Gureasko J, Kuchment O, Makino DL, Sondermann H, Bar-Sagi D, Kuriyan J. Role of the histone domain in the autoinhibition and activation of the Ras activator Son of Sevenless. *Proc Natl Acad Sci U S A*. 2010;107:3430-5.

19. Sondermann H, Soisson SM, Boykevisch S, Yang SS, Bar-Sagi D, Kuriyan J. Structural analysis of autoinhibition in the Ras activator Son of sevenless. *Cell*. 2004;119:393-405.

20. Lepri F, De Luca A, Stella L, Rossi C, Baldassarre G, Pantaleoni F, Cordeddu V, Williams BJ, Dentici ML, Caputo V, et al. SOS1 mutations in Noonan syndrome: molecular spectrum, structural insights on pathogenic effects, and genotype-phenotype correlations. *Hum Mutat*. 2011;32:760-72.

21. Li N, Batzer A, Daly R, Yajnik V, Skolnik E, Chardin P, Bar-Sagi D, Margolis B, Schlessinger J. Guanine-nucleotide-releasing factor hSos1 binds to Grb2 and links receptor tyrosine kinases to Ras signalling. *Nature*. 1993;363:85-8.

22. Chen RH, Corbalan-Garcia S, Bar-Sagi D. The role of the PH domain in the signal-dependent membrane targeting of Sos. *EMBO J*. 1997;16:1351-9.

23. Margarit SM, Sondermann H, Hall BE, Nagar B, Hoelz A, Pirruccello M, Bar-Sagi D, Kuriyan J. Structural evidence for feedback activation by Ras.GTP of the Ras-specific nucleotide exchange factor SOS. *Cell*. 2003;112:685-95.

24. Morales A, Kinnamon DD, Jordan E, Platt J, Vatta M, Dorschner MO, Starkey CA, Mead JO, Ai T, Burke W, et al. Variant Interpretation for Dilated Cardiomyopathy: Refinement of the American College of Medical Genetics and Genomics/ClinGen Guidelines for the DCM Precision Medicine Study. *Circ Genom Precis Med*. 2020;13:e002480.

25. Richards S, Aziz N, Bale S, Bick D, Das S, Gastier-Foster J, Grody WW, Hegde M, Lyon E, Spector E, et al. Standards and guidelines for the interpretation of sequence variants: a joint consensus recommendation of the American College of Medical Genetics and Genomics and the Association for Molecular Pathology. *Genet Med*. 2015;17:405-23.

26. Longoni M, Moncini S, Cisternino M, Morella IM, Ferraiuolo S, Russo S, Mannarino S, Brazzelli V, Coi P, Zippel R, et al. Noonan syndrome associated with both a new Jnk-activating familial SOS1 and a de novo RAF1 mutations. *Am J Med Genet A*. 2010;152A:2176-84.

27. Vo U, Vajpai N, Flavell L, Bobby R, Breeze AL, Embrey KJ, Golovanov AP. Monitoring Ras Interactions with the Nucleotide Exchange Factor Son of Sevenless (Sos) Using Site-specific NMR Reporter Signals and Intrinsic Fluorescence. *J Biol Chem*. 2016;291:1703-18.

28. Hall BE, Yang SS, Boriack-Sjodin PA, Kuriyan J, Bar-Sagi D. Structure-based mutagenesis reveals distinct functions for Ras switch 1 and switch 2 in Sos-catalyzed guanine nucleotide exchange. *J Biol Chem*. 2001;276:27629-37.

29. Evelyn CR, Duan X, Biesiada J, Seibel WL, Meller J, Zheng Y. Rational design of small molecule inhibitors targeting the Ras GEF, SOS1. *Chem Biol*. 2014;21:1618-28.

30. van den Berghe N, Cool RH, Wittinghofer A. Discriminatory residues in Ras and Rap for guanine nucleotide exchange factor recognition. *J Biol Chem*. 1999;274:11078-85.

31. Maurer T, Garrenton LS, Oh A, Pitts K, Anderson DJ, Skelton NJ, Fauber BP, Pan B, Malek S, Stokoe D, et al. Small-molecule ligands bind to a distinct pocket in Ras and inhibit SOS-mediated nucleotide exchange activity. *Proc Natl Acad Sci U S A*. 2012;109:5299-304.

32. Freedman TS, Sondermann H, Friedland GD, Kortemme T, Bar-Sagi D, Marqusee S, Kuriyan J. A Ras-induced conformational switch in the Ras activator Son of sevenless. *Proc Natl Acad Sci U S A*. 2006;103:16692-7.

33. Smith MJ, Neel BG, Ikura M. NMR-based functional profiling of RASopathies and oncogenic RAS mutations. *Proc Natl Acad Sci U S A*. 2013;110:4574-9.

34. McDonald CB, Bhat V, Kurouski D, Mikles DC, Deegan BJ, Seldeen KL, Lednev IK, Farooq A. Structural landscape of the proline-rich domain of Sos1 nucleotide exchange factor. *Biophys Chem*. 2013;175-176:54-62.

35. Lee YK, Low-Nam ST, Chung JK, Hansen SD, Lam HYM, Alvarez S, Groves JT. Mechanism of SOS PR-domain autoinhibition revealed by single-molecule assays on native protein from lysate. *Nature Communications*. 2017;8:15061.

36. Zarich N, Oliva JL, Martinez N, Jorge R, Ballester A, Gutierrez-Eisman S, Garcia-Vargas S, Rojas JM. Grb2 is a negative modulator of the intrinsic Ras-GEF activity of hSos1. *Mol Biol Cell*. 2006;17:3591-7.

37. Chatzifrangkeskou M, Yadin D, Marais T, Chardonnet S, Cohen-Tannoudji M, Mougenot N, Schmitt A, Crasto S, Di Pasquale E, Macquart C, et al. Cofilin-1 phosphorylation catalyzed by ERK1/2 alters cardiac actin dynamics in dilated cardiomyopathy caused by lamin A/C gene mutation. *Hum Mol Genet*. 2018;27:3060-3078.

38. Takeishi Y, Huang Q, Abe J, Che W, Lee JD, Kawakatsu H, Hoit BD, Berk BC, Walsh RA. Activation of mitogen-activated protein kinases and p90 ribosomal S6 kinase in failing human hearts with dilated cardiomyopathy. *Cardiovasc Res*. 2002;53:131-7.

39. Haq S, Choukroun G, Lim H, Tymitz KM, del Monte F, Gwathmey J, Grazette L, Michael A, Hajjar R, Force T, et al. Differential activation of signal transduction pathways in human hearts with hypertrophy versus advanced heart failure. *Circulation*. 2001;103:670-7.

40. Tajan M, Batut A, Cadoudal T, Deleruyelle S, Le Gonidec S, Saint Laurent C, Vomscheid M, Wanecq E, Treguer K, De Rocca Serra-Nedelec A, et al. LEOPARD syndrome-associated SHP2 mutation confers leanness and protection from diet-induced obesity. *Proc Natl Acad Sci U S A*. 2014;111:E4494-503.

41. Araki T, Chan G, Newbigging S, Morikawa L, Bronson RT, Neel BG. Noonan syndrome cardiac defects are caused by PTPN11 acting in endocardium to enhance endocardial-mesenchymal transformation. *Proc Natl Acad Sci U S A*. 2009;106:4736-41.

42. Kurose A, Oyama K, Murakami Y, Ohyama K, Segawa I, Sawai T. Dilated cardiomyopathy in Noonan's syndrome: a first autopsy case. *Hum Pathol*. 2000;31:764-7.

43. Shimizu A, Oku Y, Matsuo K, Hashiba K. Hypertrophic cardiomyopathy progressing to a dilated cardiomyopathy-like feature in Noonan's syndrome. *Am Heart J*. 1992;123:814-6.

44. Yu CM, Chow LT, Sanderson JE. Dilated cardiomyopathy in Noonan's syndrome. *Int J Cardiol*. 1996;56:83-5.

45. Chen PC, Wakimoto H, Conner D, Araki T, Yuan T, Roberts A, Seidman C, Bronson R, Neel B, Seidman JG, et al. Activation of multiple signaling pathways causes developmental defects in mice with a Noonan syndrome-associated Sos1 mutation. *J Clin Invest.* 2010;120:4353-65.

46. Wu X, Simpson J, Hong JH, Kim KH, Thavarajah NK, Backx PH, Neel BG, Araki T. MEK-ERK pathway modulation ameliorates disease phenotypes in a mouse model of Noonan syndrome associated with the Raf1(L613V) mutation. *J Clin Invest*. 2011;121:1009-25.

47. Araki T, Mohi MG, Ismat FA, Bronson RT, Williams IR, Kutok JL, Yang W, Pao LI, Gilliland DG, Epstein JA, et al. Mouse model of Noonan syndrome reveals cell type- and gene dosage-dependent effects of Ptpn11 mutation. *Nat Med*. 2004;10:849-57.

48. Davis J, Davis LC, Correll RN, Makarewich CA, Schwanekamp JA, Moussavi-Harami F, Wang D, York AJ, Wu H, Houser SR, et al. A Tension-Based Model Distinguishes Hypertrophic versus Dilated Cardiomyopathy. *Cell*. 2016;165:1147-1159.

49. Kehat I, Davis J, Tiburcy M, Accornero F, Saba-El-Leil MK, Maillet M, York AJ, Lorenz JN, Zimmermann WH, Meloche S, et al. Extracellular signal-regulated kinases 1 and 2 regulate the balance between eccentric and concentric cardiac growth. *Circ Res*. 2011;108:176-83.

50. Yin JC, Platt MJ, Tian X, Wu X, Backx PH, Simpson JA, Araki T, Neel BG. Cellular interplay via cytokine hierarchy causes pathological cardiac hypertrophy in RAF1-mutant Noonan syndrome. *Nat Commun*. 2017;8:15518.

51. Thum T, Gross C, Fiedler J, Fischer T, Kissler S, Bussen M, Galuppo P, Just S, Rottbauer W, Frantz S, et al. MicroRNA-21 contributes to myocardial disease by stimulating MAP kinase signalling in fibroblasts. *Nature*. 2008;456:980-4.

52. Lauriol J, Cabrera JR, Roy A, Keith K, Hough SM, Damilano F, Wang B, Segarra GC, Flessa ME, Miller LE, et al. Developmental SHP2 dysfunction underlies cardiac hypertrophy in Noonan syndrome with multiple lentigines. *J Clin Invest*. 2016;126:2989-3005.

53. Josowitz R, Mulero-Navarro S, Rodriguez NA, Falce C, Cohen N, Ullian EM, Weiss LA, Rauen KA, Sobie EA, Gelb BD. Autonomous and Non-autonomous Defects Underlie Hypertrophic Cardiomyopathy in BRAF-Mutant hiPSC-Derived Cardiomyocytes. *Stem Cell Reports*. 2016;7:355-369.

54. Carniel E, Taylor MR, Sinagra G, Di Lenarda A, Ku L, Fain PR, Boucek MM, Cavanaugh J, Miocic S, Slavov D, et al. Alpha-myosin heavy chain: a sarcomeric gene associated with dilated and hypertrophic phenotypes of cardiomyopathy. *Circulation*. 2005;112:54-9.

55. Hershberger RE, Norton N, Morales A, Li D, Siegfried JD, Gonzalez-Quintana J. Coding sequence rare variants identified in MYBPC3, MYH6, TPM1, TNNC1, and TNNI3 from 312

patients with familial or idiopathic dilated cardiomyopathy. *Circ Cardiovasc Genet*. 2010;3:155-61.

56. Kinnamon DD, Morales A, Bowen DJ, Burke W, Hershberger RE, Consortium* DCM. Toward Genetics-Driven Early Intervention in Dilated Cardiomyopathy: Design and Implementation of the DCM Precision Medicine Study. *Circ Cardiovasc Genet*. 2017;10.

Table 1. Summary of genetic findings.

Pedigree	Gene	Chr	Transcript	Genomic Position GRCh37 (hg19)	Nucleotide Change	Amino Acid Change	Max ExAC MAF*	Max gnomAD MAF*	dbSNP	Variant Classification†
A	SOS1	2	NM_005633.3	39281904	c.571G>A	p.(Glu191Lys)	0	0.0001147 (AFR)(G)	rs886041241	VUS
	FLNC	7	NM_001458.4	128489028	c.4926_4927 insACGTCACA	p.(Val1643Thrfs*26)	0	0.000009182 (NFE)(E)	Not found	LP
	TTN	2	NM_001267550.2	179413874	c.92478dupA	p.(Val30827Serfs*22)	0	0	Not found	LP
B	SOS1	2	NM_005633.3	39249749	c.1820T>C	p.(Ile607Thr)	0.00003006 (NFE)	0.00002654 (NFE)(E)	rs758699499	VUS
		2	NM_005633.3	39233616	c.2728G>C	p.(Asp910His)	0.00006061 (SAS)	0.00009806 (SAS)(E)	rs369277679	VUS
C	SOS1	2	NM_005633.3	39240612	c.2156G>C	p.(Gly719Ala)	0.0005556 (NFE)	0.0003426 (NFE)(E+G)	rs200794965	VUS
D	SOS1	2	NM_005633.3	39239427	c.2230A>G	p.(Arg744Gly)	0	0	Not found	VUS
E	SOS1	2	NM_005633.3	39213366	c.3601C>T	p.(Arg1201Trp)	0.00006058 (SAS)	0.00003266 (SAS)(E)	rs752395541	VUS
	MYH6	14	NM_002471.3	23853739	c.5476_5477 delGGinsAA	p.(Gly1826Asn)	0	0	rs878854502	VUS

*The maximum non-founder minor allele frequency (MAF) and associated population for each variant is reported. A MAF of 0 implies absence of the variant from Exome Aggregation Consortium (ExAC) / Genome Aggregation Database (gnomAD) and sufficient coverage of the genomic position. Reported gnomAD results include both exomes (E) and genomes (G) when available. AFR, African; NFE, non-Finnish European; SAS, South Asian

†Variants were adjudicated using the DCM Consortium and DCM Precision Medicine approach to DCM variant interpretation[24], refined from current American College of Medical Genetics (ACMG) / ClinGen guidelines[25]

Table 2. Clinical characteristics of study participants.

Individual	DCM	Age of Onset (y)	Age at Echo (y)	Height (cm)	LVIDD	Z-score	LVEF	ICD	Hrt. Tx.	Arrhyth.	Vital Status (Age in y, or age at death or heart transplant)	Comments / Additional Features
Pedigree A												
A.1	n/a	n/a	n/a	n/a	n/a	n/a	n/a	n/a	n/a	n/a	Deceased (d.88, unk.)	No medical records, diabetes (reported), HTN (reported)
A.2	Yes	n/a	n/a	n/a	n/a	n/a	n/a	n/a	n/a	n/a	Deceased (d. 58, HF)	No medical records, reported affected
A.3	Yes	33	77	160	65	5.601031	52.5	No	No	Yes	Alive (61)	
A.4	Yes	44	72	175	62	3.036178	25	No	No	Yes	Deceased (d.57, DCM, HF)	Degenerative arthritis, gout, migraines, cholecystectomy
A.5	No	n/a	n/a	174	55	2.315058	60	No	No	No	Alive (64)	
A.6	No	n/a	n/a	181.61	54	0.709736	47.5	No	No	Yes	Alive (42)	HTN
A.7	Yes	22	22	183	63.5	3.011836	20	Yes	Yes	Yes	Heart transplant (31)	Cardiorenal syndrome
A.8	Yes	14	14	165.1	75	6.30143	n/a	Yes	Yes	No	Deceased (d. 22), Heart transplant (14)	
Pedigree B												
B.1	n/a	n/a	n/a	n/a	n/a	n/a	n/a	n/a	No	No	Deceased (d.74, HF)	HTN (reported)
B.2	n/a	n/a	n/a	n/a	n/a	n/a	n/a	No	No	No	Deceased (d.>89y, aortic dissection)	Alzheimer's, HTN, cardiomegaly, coronary artery calcifications
B.3	Yes	56	66	170.2	66	5.358739	17	Yes	No	No	Alive (76)	Hx doxorubicin, diabetes, hyperthyroid
B.4	Yes	61	63	162.6	57	3.406839	25	Yes	No	Yes	Alive (75)	Asthma, hx 2mm circumflex coronary aneurysm
B.5	n/a	n/a	n/a	n/a	n/a	n/a	n/a	No	No	No	Deceased (d. 79, unk.)	
B.6	Yes	45	45	175.26	71	5.002545	42.5	Yes	No	No	Alive (54)	WPW, diabetes
B.7	No	n/a	n/a	n/a	n/a	n/a	n/a	No	No	No	Alive (53)	HTN, migraines, hysterectomy

Pedigree C												
C.1	Yes	69	69	n/a	78	n/a	n/a	No	No	Yes	Deceased (d.70, HF)	
C.2	No	n/a	n/a	n/a	n/a	n/a	n/a	n/a	n/a	n/a	n/a	No Medical Records
C.3	Yes	35	45	175.26	59	3.364278	40	No	No	No	Alive (57)	HTN, hypothyroid
C.4	Yes	25	25	167.64	54	2.31695	25	Yes	No	Yes	Alive (54)	MVP repair, breast neurofibromas, esophagitis, anemia
C.5	No	n/a	n/a	n/a	n/a	n/a	n/a	n/a	n/a	n/a	Alive (unk.)	No medical records
C.6	Yes	35	35	n/a	n/a	n/a	n/a	No	No	Yes	Deceased (d.42, SCD)	No medical records, reported affected
C.7	Yes	22	22	n/a	n/a	n/a	20	No	No	Yes	Alive (30)	No medical records, reported affected
Pedigree D												
D.1	n/a	n/a	n/a	n/a	n/a	n/a	n/a	n/a	n/a	n/a	Deceased (unk.)	No medical records
D.2	n/a	n/a	n/a	n/a	n/a	n/a	n/a	n/a	n/a	n/a	Deceased (unk.)	No medical records
D.3	n/a	n/a	n/a	n/a	n/a	n/a	n/a	n/a	n/a	n/a	Deceased (unk.)	No medical records
D.4	n/a	n/a	n/a	n/a	n/a	n/a	n/a	n/a	n/a	n/a	Alive (unk.)	No medical records
D.5	Yes	35	35	144	70	7.591059	27.5	No	No	No	Deceased (d.49, unk.)	
Pedigree E												
E.1	n/a	n/a	n/a	n/a	n/a	n/a	n/a	n/a	n/a	n/a	Deceased (d.80)	No medical records
E.2	n/a	n/a	n/a	n/a	n/a	n/a	n/a	n/a	n/a	n/a	Deceased (d.80)	No medical records
E.3	n/a	n/a	n/a	n/a	n/a	n/a	n/a	n/a	n/a	n/a	Alive (unk.)	No medical records
E.4	Yes	60	60	158.75	55	3.031521	25	No	No	Yes	Alive (77)	
E.5	n/a	n/a	n/a	n/a	n/a	n/a	n/a	n/a	n/a	n/a	Alive (unk.)	No medical records
E.6	Yes	47	59	172.72	70	6.170558	20	Yes	No	Yes	Deceased (d.75, unk.)	Cataracts, cholecystectomy, bladder suspension
E.7	No	n/a	n/a	178	47.7	-1.86712	66	No	No	No	Alive (53)	
E.8	No	n/a	n/a	157.48	48	0.950447	50	No	No	No	Alive (49)	

Abbreviations: Arrhyth, arrhythmia; DCM, dilated cardiomyopathy; HF, heart failure; Hrt Tx, heart transplant; HTN, hypertension; Hx, history; ICD, implantable cardioverter defibrillator; LVEF, left ventricular ejection fraction; LVIDD, LV internal dimension in diastole; MVP, mitral valve prolapse; n/a, not applicable; SCD, sudden cardiac death; unk, unknown; WPW, Wolff-Parkinson-White Syndrome.

Figure Legends:

Figure 1. DCM pedigrees with *SOS1* variants. Affection status was categorized using an ordinal grading scale. 0 (no cardiovascular disease or evidence of DCM), I (either left ventricular enlargement, LVE, without systolic function or systolic dysfunction without LVE), II (asymptomatic DCM), III (symptomatic DCM with or without medical therapy), IV (DCM requiring advanced interventions or resulting in DCM-related death). In all pedigrees, squares represent males, circles females. Diagonal lines indicate deceased individuals. Presence (+) or absence (-) of identified rare variants are indicated. Individuals for whom exome sequencing was completed are marked with an "E".

Figure 2. SOS1 activity is governed by complex interactions between six distinct functional domains. (A) SOS1 activity is natively suppressed by a primary auto-inhibitory unit comprised of the N-terminal histone-like fold (HF), Dbl homology (DH) domain, and pleckstrin homology (PH) domains and by secondary mechanisms facilitated by the proline-rich (PR) tail. This closed conformation blocks access of RAS to dual binding sites in the SOS1 catalytic core, comprised of the RAS-exchange motif (REM) and CDC25 domain. (B) Growth factor binding facilitates activation of receptor tyrosine kinases (RTKs) and recruitment of SOS1 to the membrane via direct interaction of the PR tail with GRB2, itself bound to phosphorylated tyrosine residues on the activated RTKs. Secondary membrane associations are further provided by the HF and PH domains via phosphatidylinositol 4,5-bisphosphate (PIP_2) and phosphatidic acid (PA). Alleviation of repression by these interactions permit RAS binding to a distal binding site in the REM, initiating additional allosteric changes that recruit a second RAS molecule to the adjacent

CDC25 catalytic site. Following GDP/GTP exchange, SOS1 remains strongly associated with the membrane, facilitating recruitment and activation of additional RAS molecules. (C) Simplified overview of RAS signaling pathways and associated disease phenotypes. Solid arrows represent individual steps in the ERK signaling cascade. Hatched arrows represent steps in alternate RAS-mediated AKT and JNK signaling pathways. Disease phenotypes associated with activating variants in individual pathway components are listed in italics. Affected genes are indicated in brackets. Additional abbreviations: CFC, Cardiofaciocutaneous syndrome; CS, Costello syndrome; DCM, Dilated cardiomyopathy; HCM, Hypertrophic cardiomyopathy; HGF, Hereditary gingival fibromatosis; MAP2K, Mitogen-activated protein kinase kinase; MAP3K, Mitogen-activated protein kinase kinase kinase, NS, Noonan syndrome; NSML, Noonan syndrome with multiple lentigines.

Figure 3. DCM-associated *SOS1* variants exhibit gain of function effects on MAPK/ERK signaling. HEK293T cells expressing variant or wild-type (WT) *SOS1* were serum starved for 16 hours and alternatively stimulated for 15 minutes with epidermal growth factor (EGF) (15) or left unstimulated (0). (A) Representative immunoblots for each *SOS1* variant are shown. Total protein isolates were probed using antibodies specific to phosphorylated ERK (pERK, Cell Signaling #4695, 1:5,000), total ERK (ERK, Cell Signaling #4370, 1:5,000) and SOS1 (Abcam ab140621, 1:10,000). Levels of β-tubulin were used to control for loading (Abcam, ab6046, 1:20,000). Note that pERK and total ERK levels were determined using separate blots generated from equal quantities of the same protein lysate. For figure clarity, SOS1 and β-tubulin are shown for only the pERK blot. Full blots can be found in Figure S3. (B) Differences in ERK activation between each variant and WT *SOS1* are shown as estimated ratios of median protein

expression (variant/WT) at baseline (no-EGF) and 15 min EGF stimulation. Bars represent point estimates of this ratio from a linear mixed model fit to data from three independent experimental replicates for each variant, and error bars represent pointwise 95% confidence intervals for this ratio. *, **, and *** denote two-sided $p \leq 0.05$, 0.01, and 0.001, respectively, for the null hypothesis that this ratio was 1. Relative to WT *SOS1*, elevated pERK expression was observed for both NS-associated variants used as positive ERK activation controls (M269R, E846K), as well as for all six DCM-associated *SOS1* variants. ERK activation for a suspected benign variant detected in our cohort (L791I) did not differ from WT. Differences in pERK expression were not attributable to changes in total ERK or SOS1 expression levels.

Figure 4. SOS1 gene and protein structure. The SOS1 gene and protein structure is shown. SOS1 is encoded by 22 exons spanning a total of 1333 amino acids and 6 functional domains roughly divided into two functional halves by a short helical linker. Positions and disease associations of reported *SOS1* variants are indicated. DCM-associated variants identified in this study are indicated and summarized in Table 1. SOS1 natively exists in an auto-inhibited state that is regulated by a primary N-terminal regulatory unit comprised of a histone-like fold (HF) domain, a Dbl homology (DH) domain, and a pleckstrin homology (PH) domain. Together these domains prevent RAS binding and activation at the C-terminal domains when SOS1 is not actively bound at the plasma membrane. Membrane association is primarily carried out by the proline rich (PR) tail through direct interactions with SH3 domains of GRB2. Two other C-terminal domains, a RAS-exchange motif (REM) and a CDC25 domain, together act as the catalytic core of the SOS1 protein. Alleviation of auto-inhibition following membrane association frees the REM to bind to RAS. Conformational changes promote binding of a second RAS molecule at the adjacent

CDC25 catalytic site initiating GDP/GTP exchange and RAS activation. Abbreviations: ASD, Atrial septal defect; CFC, Cardiofaciocutaneous syndrome; HCM, hypertrophic cardiomyopathy; HGF, hereditary gingival fibromatosis; NS, Noonan syndrome.

Figure 5. (A) SOS1 domain organization (PDB: 3KSY). Positions of DCM-associated variants identified in this study are indicated. Hatched bars indicate approximate allosteric and catalytic RAS binding sites. (B) Modeling of the wild-type SOS1 suggests the presence of an intermittent electrostatic association between Glu191 and Lys420 (evidenced by multiple short-lived 4 Å distance measurements) that is absent in models of p.(Glu191Lys). (C) Modeling of p.(Ile607Thr) suggests a hydrogen bond rearrangement between the region surrounding Ile607 and the neighboring CDC25 helical hairpin . The addition of an –OH group promotes interactions between both Arg576-Thr607 and Lys953-Thr607 (left) and reorients the CDC25 helical hairpin closer to the REM domain (right). The bar graph displays reduced average distance from the end of the sidechain of Lys953 to Thr607. Average distances with standard deviations represent 1100 independent measurements compiled over 25ns (D) p.(Gly719Ala) is positioned between the allosteric and catalytic RAS binding sites. Other amino acids within this same helix are involved in allosteric changes to the REM domain following RAS binding[27]. (E) Modeling of p.(Arg744Gly) demonstrates a localized unwinding of the surrounding helix by about 1 turn. (F) Asp910 is located at the SOS1-RAS interface and directly associates with Arg41 of the RAS Switch 1 region[28].

Pedigree A - SOS1 E191K (S), FLNC V1643TfsTer26 (F),TTN V30827SfsTer22 (T)

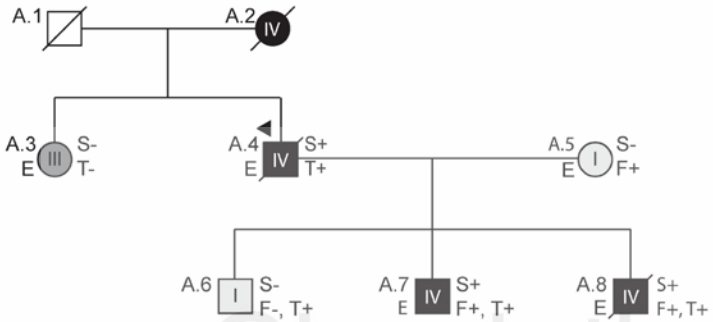

Pedigree B - SOS1 I607T (S1), SOS1 D910H (S2)

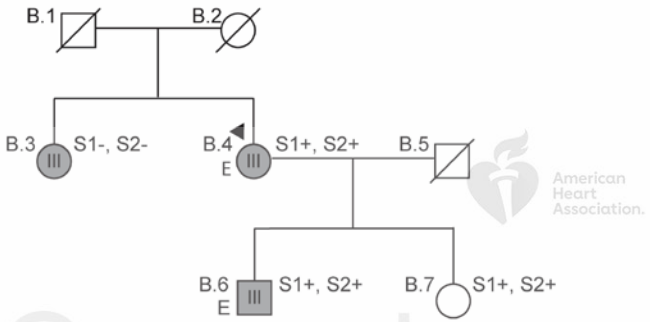

Pedigree C - SOS1 G719A (S)

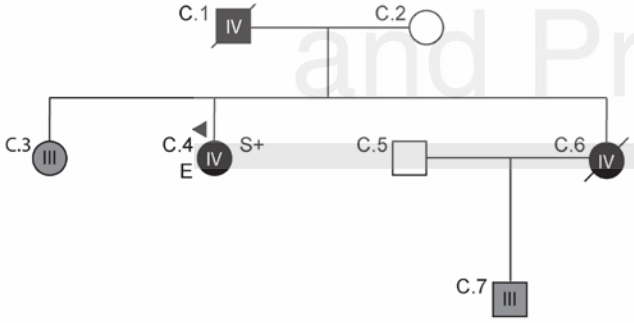

Pedigree D - SOS1 R744G (S)

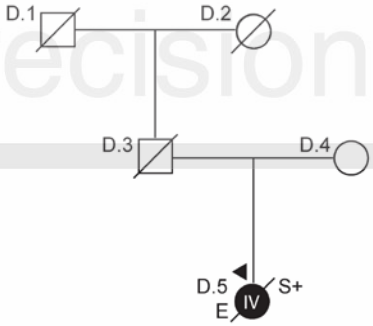

Pedigree E - SOS1 R1201W (S), MYH6 G1826N (M)

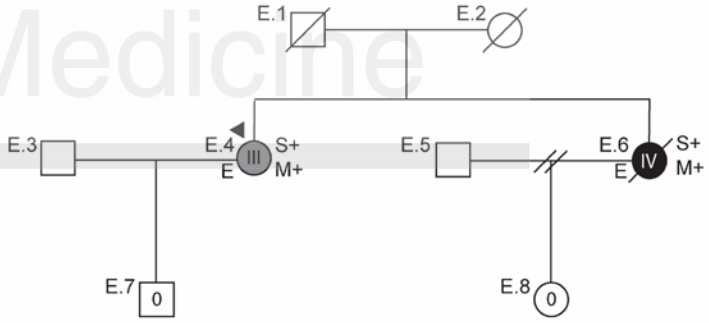

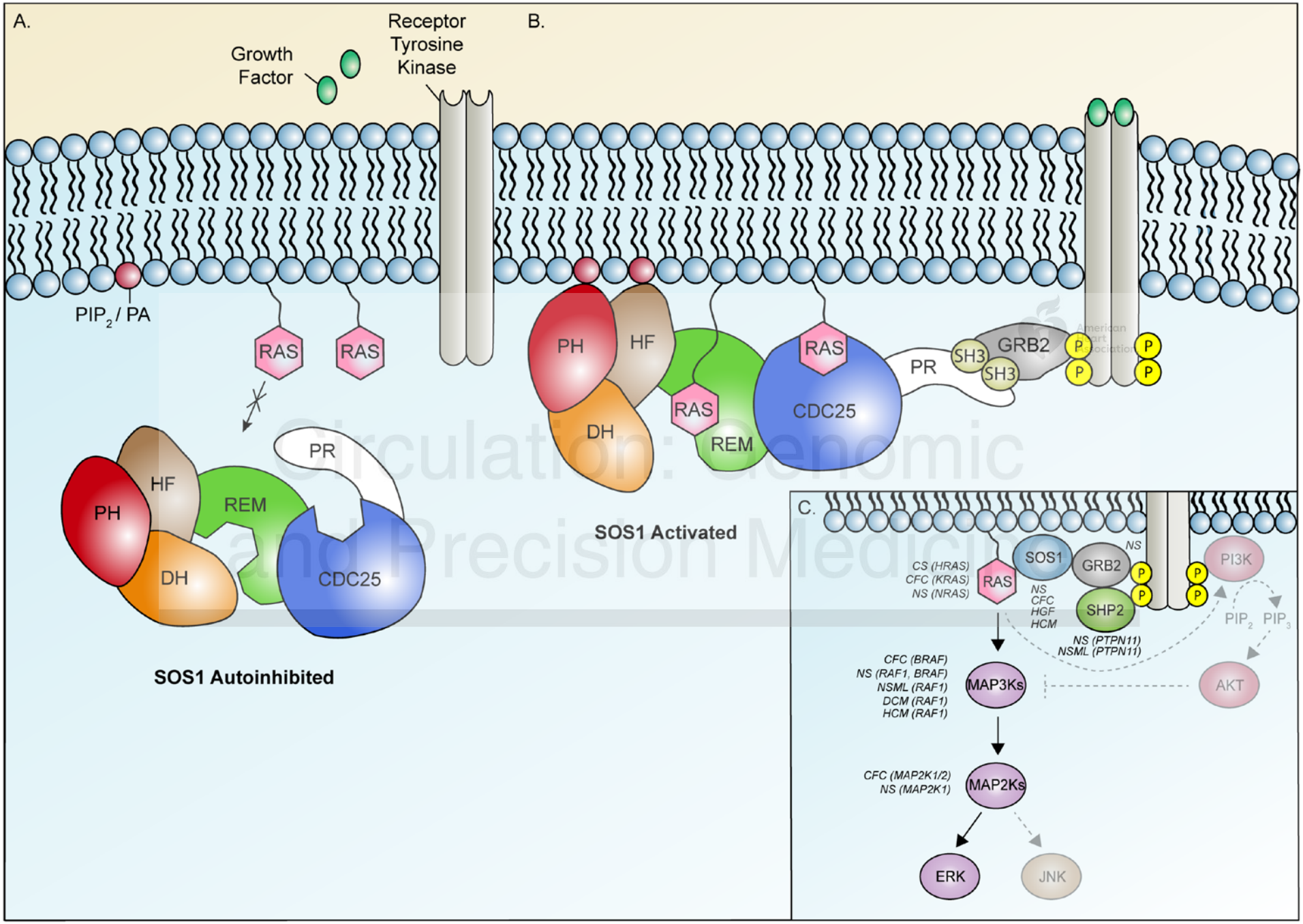
A.
Growth Factor
Receptor Tyrosine Kinase
B.
PIP2 / PA
RAS
RAS
PH
HF
REM
DH
CDC25
PR
SOS1 Autoinhibited
RAS
PH
HF
DH
REM
RAS
CDC25
PR
SH3
SH3
GRB2
P
SOS1 Activated
C.
CS (HRAS)
CFC (KRAS)
NS (NRAS)
RAS
SOS1
GRB2
NS
SHP2
NS
CFC
HGF
HCM
NS (PTPN11)
NSML (PTPN11)
PI3K
PIP2
PIP3
AKT
CFC (BRAF)
NS (RAF1, BRAF)
NSML (RAF1)
DCM (RAF1)
HCM (RAF1)
MAP3Ks
CFC (MAP2K1/2)
NS (MAP2K1)
MAP2Ks
ERK
JNK

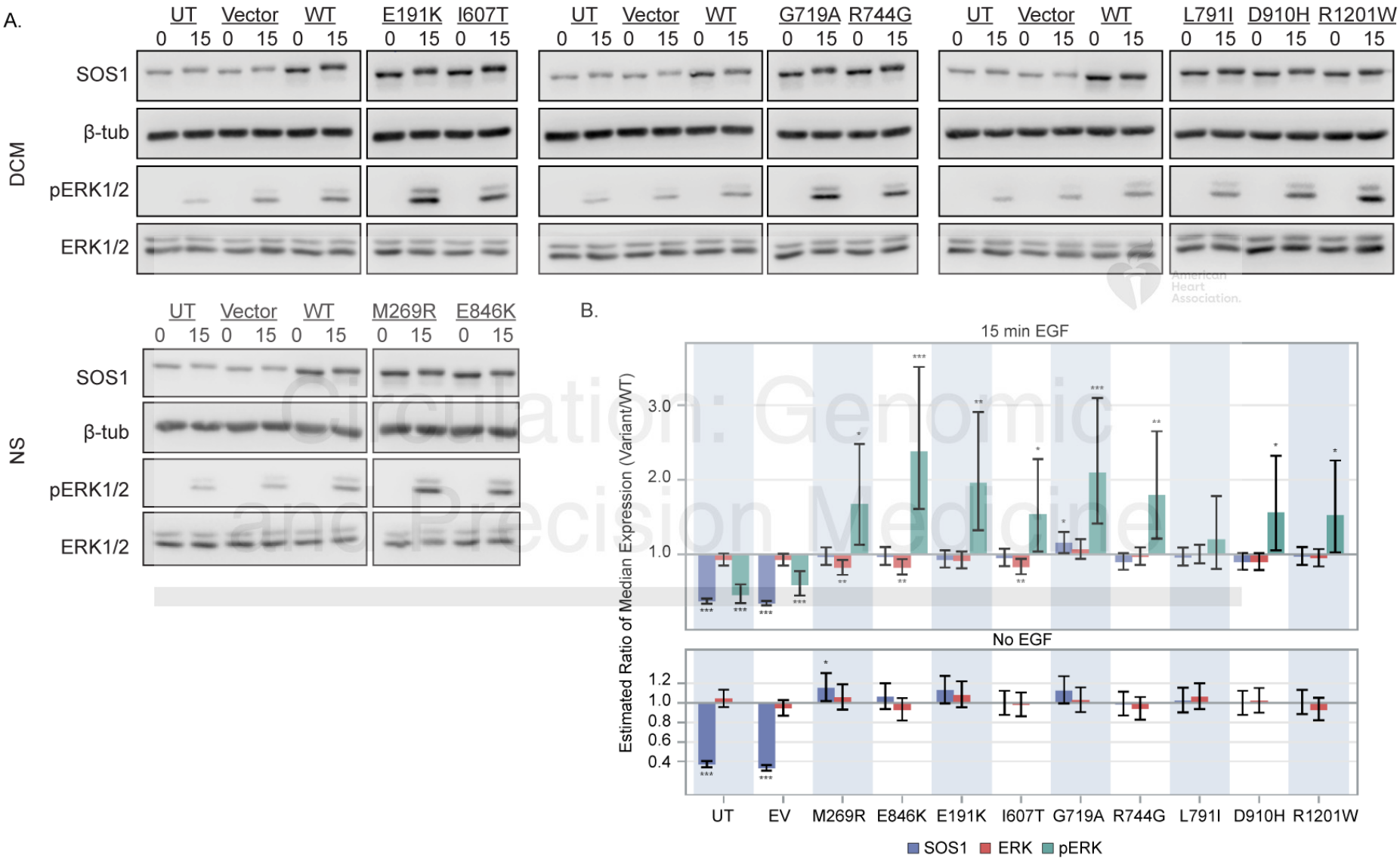

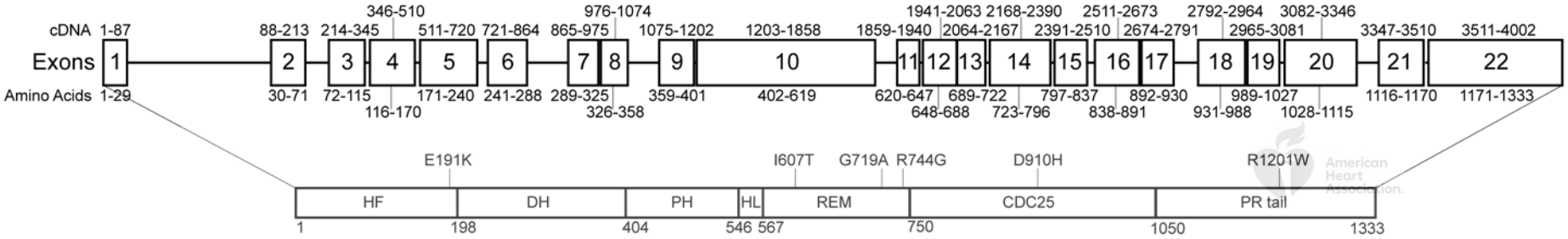

Histone Fold (HF)	
F78C	NS
P102R	NS
E108K	NS
P112R	NS
T158A	CFC
K170E	NS

Dextrin Homology (DH)	
R248C	NS
I252T	NS
T266K	NS
M269T	NS
M269R	NS/HCM
D309Y	NS
Y337C	NS
P340S	NS

Plextrin Homology (PH)	
K427_D430delinsD	NS
D430del	NS
W432_E433del	NS
W432R	NS
E433K	NS
G434K	NS
G434R	NS
I437N	NS
I437T	NS
C441Y	NS
Q477H	NS
Q477R	NS
P478L	NS
P478R	NS
P481_G482insRLP	CFC
G482R	NS
L490R	NS
R497Q	NS
Glu533K	ASD

Helical Linker (HL)	
S548R	NS
T549K	NS
L550P	NS
R552K	NS
R552T	NS
R552S	NS/CFC
R552M	NS
R552G	NS
L554_M558delinK	NS

Ras Exchange Motife (REM)	
D620_P621insH	NS
F623I	NS
V624F	HCM
P655L	NS
Y702H	NS
K728I	NS
W729L	NS
I733N	NS
I733F	NS

CDC25	
E846K	NS/CFC/HCM
P894R	NS
Q977R	NS
P1045R	NS

Proline-rich (PR) tail	
R1084fs*1105	HGF
S1096T	HCM